

## Search for pulsed $\gamma$ -ray emission from radio pulsars in the COS-B data

R. Buccheri<sup>3</sup>, K. Bennett<sup>6</sup>, G. F. Bignami<sup>2</sup>, J. B. G. M. Bloemen<sup>1,\*</sup>, V. Boriakoff<sup>7</sup>, P. A. Caraveo<sup>2</sup>, W. Hermsen<sup>1</sup>, G. Kanbach<sup>4</sup>, R. N. Manchester<sup>8</sup>, J. L. Masnou<sup>5</sup>, H. A. Mayer-Hasselwander<sup>4</sup>, M. E. Özel<sup>4,\*\*</sup>, J. A. Paul<sup>5</sup>, B. Sacco<sup>3</sup>, L. Scarsi<sup>3</sup>, and A. W. Strong<sup>2</sup>

The Caravane Collaboration

<sup>1</sup> Cosmic Ray Working Group, Huygens Laboratorium Leiden, The Netherlands

<sup>2</sup> Istituto di Fisica Cosmica del C.N.R., Milano, Italy

<sup>3</sup> Istituto di Fisica Cosmica e Informatica del C.N.R., I-90139 Palermo, Italy

<sup>4</sup> Max-Planck-Institut für Physik und Astrophysik, Institut für Extraterrestrische Physik, D-8046 Garching bei München, Federal Republic of Germany

<sup>5</sup> Service d'Astrophysique, Centre d'Etudes Nucleaires de Saclay, F-91191 Gif-sur-Yvette, France

<sup>6</sup> Space Science Department, European Space Agency, Noordwijk, The Netherlands

<sup>7</sup> N.A.I.C. – Cornell University – Ithaca, New York

<sup>8</sup> CSIRO, Division of Radiophysics, Sydney, Australia

Received April 25, accepted July 5, 1983

**Summary.** Pulsar parameters relating to 145 radio observations contemporary with  $\gamma$ -ray observations by COS-B have been used to search for pulsed  $\gamma$ -ray emission from radio pulsars in the energy range 50 MeV to 2 GeV. No positive signal has been detected either from any individual pulsar or globally.

In particular no  $\gamma$ -ray signal has been detected from PSR0740–28, PSR0950+08, PSR1055–52, and PSR1929+10, expected to be visible by COS-B on the basis of current models of  $\gamma$ -ray emission from pulsars. This result shows that the average product,  $\eta I$ , of the conversion efficiency  $\eta$  from the pulsar braking power into  $\gamma$ -rays and the pulsar moment of inertia  $I$ , cannot exceed  $6 \cdot 10^{43} \text{ g cm}^2$  for pulsar ages greater than 40000 yr. This implies that the contribution of old pulsars to the observed galactic  $\gamma$ -ray emission is less than 5 % for  $\gamma$ -ray energies greater than 50 MeV.

**Key words:**  $\gamma$ -rays – pulsars – COS-B

### Introduction

The search for  $\gamma$ -ray emission from pulsars is motivated from both an observational and theoretical standpoint. Two of the most conspicuous galactic  $\gamma$ -ray sources, and the only ones definitely identified with known celestial objects, are PSR0531+21 (The Crab pulsar) and PSR0833–45 (the Vela pulsar), the two “youngest” pulsars of the Manchester and Taylor catalogue (MT, 1981). Their  $\gamma$ -ray emission is pulsed at the radio period and the intensity observed can be explained by models describing the early stages of pulsar evolution.

The energy reservoir for pulsars is assumed to be the rotational energy and the observed emission at  $E_\gamma > 50 \text{ MeV}$  is a fraction of the energy loss  $\dot{E} = I\omega\dot{\omega}$  (where  $I$  is the moment of inertia of the neutron star and  $\omega$  the pulsar angular velocity). For the Crab

and Vela pulsars, the efficiency of conversion  $\eta$  from  $\dot{E}$  into  $\gamma$ -ray luminosity  $L_\gamma$  lies in the interval  $10^{-3}$ – $10^{-4}$  when  $I$  is assumed to be equal to a canonical value  $I_0 = 10^{45} \text{ g cm}^2$ . This conversion efficiency, when applied to the other pulsars of the MT catalogue, results in a predicted  $\gamma$ -ray luminosity  $L_\gamma = \eta\dot{E}$  too low to be observable by COS-B. On the other hand, some current models predict  $\eta$  to increase with pulsar age (Buccheri et al., 1978; Harding, 1981) up to values orders of magnitude greater than those of the Crab and Vela pulsars. If this were the case, several other pulsars of the MT catalogue would exceed the visibility threshold of COS-B.

This paper reports the results of a systematic search for  $\gamma$ -ray emission from radio pulsars in the COS-B data which was one of the major objectives of the COS-B mission at its conception (Van de Hulst et al., 1971). Similar searches carried out in the past with the SAS-II data and with preliminary COS-B data revealed some difficulties in interpretation of the results because of imprecision on the pulsar parameters as measured at radio wavelengths. Ögelman et al. (1976), analysing the SAS-II data, folded the  $\gamma$ -ray arrival times with pulsar periods  $P$  and period derivatives  $\dot{P}$  as extrapolated from the epochs of radio measurement to the SAS-II epoch, generally several months apart. This procedure resulted in an unpredictable loss of precision in these parameters mainly owing to pulsar period noise. To overcome this difficulty, the COS-B team, in a preliminary analysis, performed a search in a limited range of  $P$  and  $\dot{P}$  values around those extrapolated from the epochs of the radio observations (Kanbach et al., 1977; Buccheri, 1981).

Both procedures lead to questionable results. For the SAS-II analysis the positive indication for PSR0747–46 (Thompson et al., 1976) must be disregarded because of an error on the adopted value of  $\dot{P}$  (MT, 1981). The absence of conclusive evidence for  $\gamma$ -ray emission from other pulsars could also have been the consequence of insufficient precision in the pulsar parameters. For COS-B, the possible detection of PSR1822–09 and PSR0740–28 was subsequently contradicted by differences between newly measured radio periods and the derived  $\gamma$ -ray pulsar periods (Buccheri, 1981). The detected effect could have been the result of unknown instrumental periodicities present in the data and emphasized by the scanning procedure. Alternatively, an unknown physical process would have to be invoked to account for the difference between the  $\gamma$ -ray and the radio periods.

Send offprint requests to: R. Buccheri

\* Also Sterrewacht, Huygens Laboratorium, Leiden, The Netherlands

\*\* On leave from Middle East Technical University, Ankara, Turkey

In the present analysis, either strictly contemporary radio and  $\gamma$ -ray data or pulsar parameters which could be reliably derived by interpolation from radio measurements spanning the COS-B observations are used. With this approach the required precision in the pulsar parameters needed for the analysis of the COS-B data is assured. In addition to the search for emission from individual pulsars, a statistical "point summation" technique has been applied aiming at the detection of a global signal from a selected sample of pulsars.

### The data base

The  $\gamma$ -ray data (energies between 50 MeV and 2 GeV) are from 21 COS-B observations spanning almost five years from August 1975 to April 1980 (see Table 1).

The radio pulsar reference data set is the MT catalogue containing 330 entries. Two of the objects listed there, PSR0531+21 and PSR0833-45, are a case apart widely studied in the literature, and will only be used for calibration purposes. Values of  $P$  and  $\dot{P}$  have been taken from Gullahorn and Rankin (1978), Newton et al. (1981), Ferguson and Boriakoff (1980) and Manchester et al. (1983), where the time span on the radio measurements are specified. This information permits the selection of those pulsars for which the parameters have been derived during time intervals covering the COS-B observations.

Table 2 lists four pulsars for which dedicated radio observations were performed simultaneously with COS-B. The rms phase residuals are expressed as a fraction of the corresponding pulsar period and represent the average broadening of the pulse width of

the pulsar in the integrated pulse profile. The table shows that the precision in the radio measurements is sufficient for the analysis of the  $\gamma$ -ray data.

In the more general case where radio observations span the  $\gamma$ -ray observations, i.e. not strictly contemporary, the rms phase residuals are greater than those shown in Table 2. In no case do they exceed  $2 \cdot 10^{-2}$ , thus giving confidence in the use of the radio parameters.

It is, however, necessary to offer a word of caution. The values of the rms phase residuals quoted in the literature are generally obtained by analysing few tens of radio pulses collected in observations lasting several years, with an average of about one radio pulse per month. For pulsars in which the time scale of the period noise is comparable with one month (i.e. the typical duration of a COS-B observation) the effective rms phase residual could be greater than that quoted in the literature. This is the case for PSR0740-28 where the rms phase residual computed by Manchester et al. (1982) for 4 yr of data, amounts to 0.2. On the other hand, longer observations of PSR0540+23 and PSR0611+22 (Gullahorn and Rankin, 1978) and PSR1822-09 (Newton et al., 1981) have not resulted in rms phase residuals greater than those shown in Table 2.

The necessity of using contemporary radio and  $\gamma$ -ray data together with the limitation to aspect angles less than  $18^\circ$ , because of experiment sensitivity considerations (Mayer-Hasselwander et al., 1982), reduces the number of useful pulsars from 328 to 117. With the repeated observation by COS-B of various regions of the galactic disc, several pulsars have been within the COS-B field of view more than once. In particular PSR0736-40 has been in the field of view six times, PSR1641-45, PSR0540+23, and PSR1556-44 three times and 17 other pulsars have been in the field of view twice. This increases the total number of independent pulsar measurements to 145.

### The method of analysis

For each of the 145 pulsar observations, the photon arrival times were reduced to a phase value in the interval 0 to 1 by the relation

$$\phi_j = \text{fractional part of } (v_i \Delta t_{ij} + \dot{v}_i \Delta t_{ij}^2 / 2 + \ddot{v}_i \Delta t_{ij}^3 / 6) \quad (1)$$

with  $j=1, N_i$ , where  $N_i$  is the number of photons used in the case of the  $i$ th pulsar ( $i=1, 145$ ), and  $v_i$  is the pulsar frequency.

$\Delta t_{ij} = t_j - t_{0i}$  with  $t_{0i}$  radio epoch at the Solar System Barycentre,  $t_j$  arrival time (at the Solar System Barycentre) of the  $j$ th photon. The  $N_i$  phase values obtained with relation (1) were Fourier-analysed by means of the statistical variable  $Z_n^2$  defined as

$$Z_n^2 = (2/\dot{N}_i) \sum_{k=1}^n \left( \sum_{j=1}^{N_i} \cos k \phi_j \right)^2 + \left( \sum_{j=1}^{N_i} \sin k \phi_j \right)^2, \quad (2)$$

where  $n$  is the chosen number of harmonics.

The variable  $Z_n^2$  has a probability density function (p.d.f.) equal to that of a  $\chi^2$  with  $2n$  degrees of freedom (Bendat and Piersol, 1971) as does, in particular conditions, the more usual  $Y_{2n+1}^2 = \sum_i (x_i - \bar{x})^2 / \bar{x}$  based on the number of counts  $x_i$  per bin

derived by sorting the phases  $\phi_j$  into  $2n+1$  phase bins, and their average  $\bar{x}$ . The choice of  $Z_n^2$  instead of  $Y_{2n+1}^2$  is justified by the fact that the number  $N_i$  can be sometimes as low as 100. In such a case the latter variable does not have a  $\chi^2$  probability function (p.d.f.). Its use would then necessitate the derivation of the suitable p.d.f. (by Monte Carlo methods for instance) which could be different for different values of  $N_i$ .

**Table 1.** COS-B observations used in the timing analysis

obs.no.	Pointing direction		start time	end time	Useful time (days)
	$l$	$b$			
1	184	- 6.1	1975-08-17	1975-09-17	18.8
3A	263.5	- 3.3	-10-08	-11-08	12.3
3B	262.7	3.5	-11-08	-11-28	13.2
4	73.9	0.3	-11-28	-12-24	17.0
5	291.6	0.2	-12-24	1976-01-23	18.9
7	321.5	0.3	1976-02-23	-03-24	19.9
8	25.7	1.5	-03-24	-04-24	20.6
9	44.9	- 2.1	-04-24	-05-24	19.7
10	283.9	68.7	-05-24	-06-24	20.9
12	262.5	3.2	-07-24	-08-21	20.1
13	352.1	8.5	-08-21	-09-30	23.4
14	195.3	4.3	-09-30	-11-02	21.5
21	243.3	- 2.4	1977-05-02	1977-06-08	24.9
24	345.3	- 4.5	-08-18	-09-23	19.2
31	229.1	44.0	1978-05-03	1978-06-09	14.5
33	310.2	0.4	-07-17	-08-23	22.0
39	190.2	- 0.3	1979-02-22	1979-04-03	23.6
40	243.2	- 2.6	-04-03	-05-09	19.3
42	278.0	0.1	-06-20	-07-27	21.0
45	263.0	3.9	-10-10	-11-15	18.5
49	21.1	2.3	1980-02-29	1980-04-08	22.9

**Table 2.** Pulsars observed simultaneously in the radio and  $\gamma$ -ray range

PSR	COS-B Obs no.	rms phase residual	Observatory
0540+23	39	$6 \times 10^{-4}$	Arecibo
0611+22	39	$2 \times 10^{-3}$	Arecibo
0740-28	21	$2 \times 10^{-3}$	Tidbinbilla
0740-28	40	$5 \times 10^{-4}$	Tidbinbilla
1822-09	49	$2 \times 10^{-3}$	Parkes

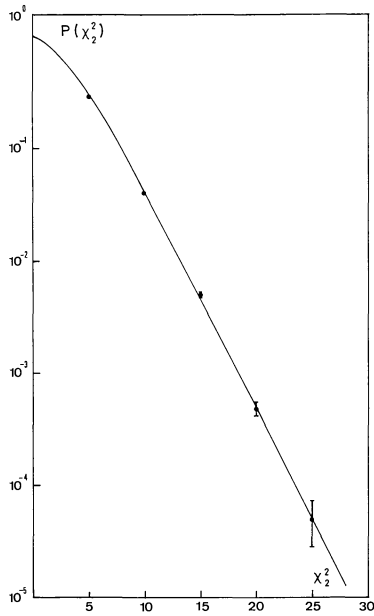


**Fig. 1.** Cumulative distribution  $P(\chi^2) = \int_{\chi^2}^{\infty} f(\chi^2) d\chi^2$ . The continuous line refers to the theoretical  $\chi^2$  with 4 d.o.f. The points derive from a simulation of the variable  $Z_2^2$  using 100 arrival times

The value  $n=2$  has been chosen to optimize the signal-to-noise ratio. In the case of very intense light curves of small duty cycle the use of a larger number of harmonics would be justified (Gerardi et al., 1982). The choice  $n=2$  has also the advantage of ensuring the correct use of the radio parameters in cases where the rms phase residual is as high as 0.2.

Figure 1 shows the  $\chi^2_4$  cumulative distribution function (theoretical) compared with the corresponding function of the variable  $Z_2^2$  as derived by Monte Carlo simulations for  $N_i=100$ . The agreement is excellent and “a fortiori” it will be so for higher values of  $N_i$ .

In the absence of pulsation the expectation value of  $Z_2^2$  is 4. When a periodic signal is present due to  $Np_i$  “pulsed” photons, the contribution to  $Z_2^2$  (in terms of number of sigmas above the average) is given by (see for example Buccheri et al., 1977)

$$n_o(\theta) = \frac{N^2 p_i(\theta)}{N_i(\theta)} C, \quad (3)$$

where  $\theta$  is the acceptance angle from the pulsar direction and the constant  $C$  depends on the duty cycle of the pulsation.

The COS-B angular resolution is a function of the energy of the incoming photons (Scarsi et al., 1977) so the saturation of  $Np_i$  is reached at lower values of  $\theta$  for higher energies. As a consequence the value of  $n_o$  will reach its maximum value at lower  $\theta$  for higher photon energies. A detailed analysis of the behaviour of  $n_o$  has been given in Buccheri et al. (1977) for a gaussian instrumental response and for flat background. In the present case, where the presence of a highly structured galactic disc strongly affects the analysis, the optimal value of  $\theta$  as a function of the photon energy has been determined empirically using the high statistics available in the cases of the Crab and Vela pulsars. By investigating the dependence of  $Z_2^2$  on the acceptance angle  $\theta$  for these two pulsars, in different energy ranges and for different

inclinations with respect to the COS-B axis, a law of the form

$$\theta_m = 12.5 \times E_{\text{MeV}}^{-0.16} \text{ degrees} \quad (4)$$

has been derived. The  $\gamma$ -ray photons of energy  $E$  (MeV) falling within  $\theta_m(E)$  have been used in our analysis.

## Results

For the 145 pulsar observations used, Table 3 lists the following: the number of the COS-B observation in which the pulsar has been observed, the sensitive area  $\varepsilon_i$  (derived assuming an  $E^{-2}$  spectrum), the number  $N_i$  of photons accepted, the pulsar period  $P$  in seconds, the value  $m_{\sigma i} = (Z_2^2 - 4)/\sqrt{8}$  and the related probability for chance occurrence  $g_i$  as derived by the distribution of Fig. 1.

The highest value of  $m_{\sigma i}$  of the lists is for PSR1309–55 and corresponds to a chance occurrence probability of  $3.1 \cdot 10^{-3}$ . PSR1309–55 is an old pulsar ( $\sim 2.3 \cdot 10^6$  yr) located at 4.8 kpc. It would become visible by COS-B only if its moment of inertia  $I$  were  $\sim 1500$  times the canonical value  $I_0$  and its rotational energy loss were entirely converted into  $\gamma$ -rays. These conditions being very unlikely (see for example Moszkowski, 1974), the effect found is attributed to a chance fluctuation to be expected from the number of independent pulsars analysed. Other large deviations of  $Z_2^2$  from the mean value are found for PSR0611+22, PSR0950–38, and PSR1907+02. Just as for PSR1309–55 the results can have arisen from chance fluctuations.

In order to see if individually undetectable signals combine to give a detectable global signal, the 145 values measured for  $g_i$  have been combined through the relation (Eadie et al., 1971)

$$\alpha = -2 \ln \prod_{i=1}^{145} g_i \quad (5)$$

resulting in  $\alpha = 305.9$ . Since the variable  $\alpha$  has a  $\chi^2_{290}$  p.d.f., the value 305.9 corresponds to a probability for chance occurrence of  $\sim 25\%$ .

Those pulsars for which the theoretical expectation for  $\gamma$ -ray visibility is highest, may be selected from the sample.

On the hypothesis that pulsed gamma radiation is emitted by pulsars in proportion to a fraction  $\eta$  of their loss of rotational energy  $\dot{E} = I\omega\dot{\omega}$ , the expected number of photons at the experiment is given by

$$Np_i = \eta \dot{E} \frac{\varepsilon_i \Delta t_i}{4\pi f d^2} \frac{1}{\langle E_\gamma \rangle}, \quad (6)$$

where  $4\pi f$  is the pulsar beaming factor (assumed to be 2.3 sr as in the cases of the Crab and Vela pulsars),  $\varepsilon_i$  and  $\Delta t_i$  refer to the sensitive area and observation time and  $\langle E_\gamma \rangle$  is the average photon energy in the interval 50 MeV to 2 GeV, (i.e.  $\sim 190$  MeV for an  $E^{-2}$  spectrum). Combining Eqs. (3) and (6) we have for the  $i^{\text{th}}$  pulsar

$$n_{\sigma i} = \frac{CR^2}{N_i \langle E_\gamma^2 \rangle} (\eta I)^2 (\omega \dot{\omega})^2 \left( \frac{\omega_i \Delta t_i}{4\pi f d^2} \right)^2, \quad (7)$$

where the factor  $R(<1)$  has been added to take into account the source counts reduction due to the size of the acceptance cone.

The value of  $CR^2$  can be estimated by applying the relation (3) to the Crab and Vela cases observed by COS-B several times. This value is, on average, 0.25 for Crab and 0.18 for Vela consistent with the greater duty cycle of Vela (Wills et al., 1981). The average value  $CR^2 = 0.22$  is used thus making the hypothesis that the light curve structure is similar to that of the Crab and Vela pulsars.

**Table 3.** List of pulsars observations

PSR	OBS n°	S(cm <sup>2</sup> )	N <sub>i</sub>	P(s)	m <sub>σi</sub>	g <sub>i</sub> %	PSR	OBS n°	S(cm <sup>2</sup> )	N <sub>i</sub>	P(s)	m <sub>σi</sub>	g <sub>i</sub> %
0525+21	1	20.2	443	3.745	0.619	21.85	1426-66	33	17.3	974	0.785	0.515	24.36
	14	9.6	227	3.745	0.603	22.22	1436-63	33	17.5	1020	0.460	-0.631	69.62
0540+23	1	19.4	486	0.246	-0.390	57.52	1449-64	33	16.4	827	0.179	-1.063	91.08
	14	12.2	273	0.246	-0.460	60.94	1451-68	7	13.6	221	0.263	0.352	28.77
	39	14.4	356	0.246	1.135	12.52		33	14.6	571	0.263	0.563	23.17
0611+22	14	17.9	305	0.335	3.093	1.26	1454-51	33	11.1	220	1.748	0.813	17.79
	39	16.3	315	0.335	-0.660	71.13	1503-51	33	10.8	260	0.841	0.053	38.61
0736-40	3A	14.2	119	0.375	-0.247	50.87	1503-66	33	14.7	521	0.356	-0.251	51.05
	3B	10.3	89	0.375	-0.517	63.79	1510-48	33	7.8	147	0.455	0.242	32.12
	12	7.8	87	0.375	0.080	37.62	1523-55	33	11.2	409	1.049	0.695	20.17
	21	12.6	152	0.375	0.163	34.72	1530-53	33	9.3	317	0.369	-1.124	93.56
	40	10.7	90	0.375	-1.137	94.06	1541-52	33	8.0	289	0.179	0.388	27.74
	45	7.6	81	0.375	1.154	12.26	1550-54	33	8.0	296	1.081	0.689	20.30
0740-28	21	21.4	326	0.167	0.277	31.02	1555-55	33	7.9	269	0.957	0.429	26.61
	40	18.0	242	0.167	-0.832	80.04	1556-44	7	11.1	231	0.257	-0.858	81.36
0818-41	40	8.5	202	0.545	-0.745	75.55		13	6.7	213	0.257	-0.940	85.43
0826-34	40	11.3	133	1.849	-0.791	77.93		24	9.7	210	0.257	1.836	5.65
0835-41	40	6.7	191	9.752	1.675	6.80	1556-57	33	8.7	264	0.194	0.352	28.77
0839-53	42	10.8	208	0.721	0.358	28.60	1557-50	7	15.7	679	0.193	-0.173	47.63
0840-48	42	9.5	383	0.644	-0.680	72.17		24	9.2	363	0.193	-1.040	90.08
0844-35	40	8.2	99	1.116	-0.951	85.96	1641-45	7	8.0	398	0.455	0.683	20.43
0855-61	42	11.6	148	0.963	-0.465	61.19		13	8.4	484	0.455	-0.400	58.00
0901-63	42	11.2	145	0.660	-0.996	88.09		24	16.4	806	0.455	1.185	11.84
0903-42	42	8.2	279	0.965	-1.094	92.37	1822-09	49	14.2	827	0.769	-0.049	42.51
0905-51	42	13.2	304	0.254	0.276	31.06	1900+05	8	8.7	429	0.747	-0.025	41.57
0909-71	42	6.2	177	1.363	-0.353	55.76		9	17.4	695	0.747	-0.173	47.63
0919+06	31	16.7	92	0.431	-0.349	55.57	1906+09	8	6.2	255	0.830	-0.717	74.09
0923-58	42	14.8	254	0.739	-0.623	69.21		9	19.2	688	0.830	-0.497	62.78
0932-52	42	15.6	354	1.445	-0.870	81.97	1907+00	8	10.7	479	1.017	-0.577	66.84
0940-55	42	16.4	383	0.664	-0.746	75.60		9	14.2	491	1.017	-0.665	71.39
0941-56	42	16.2	385	0.808	0.202	33.42	1907+02	8	9.5	454	0.495	2.427	2.81
0950-38	42	7.4	81	1.374	2.905	1.58		9	16.3	637	0.495	-0.646	70.40
0950+08	31	21.3	110	0.253	-0.546	65.26	1907+10	9	19.2	609	0.284	0.494	24.89
0953-52	42	16.6	361	0.862	-0.258	51.37	1907+12	9	19.8	557	1.442	-0.611	68.59
0957-47	42	14.2	215	0.670	0.574	22.91	1910+20	9	13.1	236	2.233	-0.411	58.54
0959-54	42	17.2	439	1.437	0.047	38.83	1911-11	9	19.6	627	0.601	-0.034	41.92
1001-47	42	13.9	199	0.307	-0.463	61.09	1911+13	9	18.3	545	0.521	-0.603	68.18
1014-53	42	16.4	387	0.770	-0.192	48.45	1913+10	9	20.0	674	0.405	-1.139	94.13
1015-56	42	16.3	462	0.503	-0.414	58.68	1913+607	9	16.7	445	1.616	1.206	11.57
1039-55	42	14.7	373	1.171	-0.173	47.63	1914+09	9	20.1	683	0.270	0.68P	20.49
1044-57	42	14.0	404	0.369	-0.265	51.68	1914+13	9	19.0	595	0.282	0.054	38.57
1054-62	42	11.5	323	0.422	-1.322	99.22	1915+13	9	18.6	581	0.195	-0.683	72.32
1055-52	42	12.8	208	0.197	0.906	16.09	1916+14	9	18.1	546	1.181	-0.352	55.71
1056-57	42	13.0	361	1.185	-0.067	43.23	1917+00	8	9.1	286	1.272	-0.362	56.18
1105-59	42	11.8	342	1.517	-0.930	84.95		9	14.7	358	1.272	0.304	30.20
1110-65	33	7.5	189	0.334	-0.706	73.52	1918+19	9	14.3	334	0.821	-0.419	58.93
	42	8.9	292	0.334	-0.941	85.48	1919+14	9	18.4	561	0.618	0.965	15.09
1110-69	33	7.5	215	0.820	-0.208	49.14	1919+21	9	12.6	240	1.337	-0.689	72.63
	42	7.2	303	0.820	-1.290	98.63	1920+21	9	13.2	271	1.078	0.876	16.62
1119-54	42	10.8	178	0.536	-0.117	45.26	1924+14	9	18.2	549	1.325	1.013	14.32
1133-55	42	9.4	162	0.365	0.474	25.41	1924+16	9	16.6	482	0.580	-0.589	67.46
1133+16	10	9.9	73	1.188	0.344	29.01	1925	4	7.8	166	1.431	0.934	15.61
1143-60	33	9.8	246	0.273	0.974	14.94		9	11.9	234	1.431	0.512	24.43
	42	8.3	276	0.273	0.921	15.83	1927+13	9	18.7	555	0.760	0.222	32.76
1154-62	33	11.3	366	0.401	0.333	29.33	1929+10	9	19.3	527	0.227	-0.262	51.55
	42	7.1	322	0.401	-0.539	64.90	1929+20	9	13.6	330	0.268	-0.742	75.39
1159-58	42	6.9	202	0.453	2.203	3.67	1930+22	4	8.2	176	0.144	-1.223	96.94
	33	10.8	228	0.453	0.450	26.04	1933+15	9	16.9	444	0.967	0.368	28.31
1221-63	33	14.1	634	0.216	0.273	31.15	1944+17	9	14.1	295	0.441	0.746	19.11
1222-63	33	14.2	646	0.420	1.504	8.27	1944+22	4	9.9	199	1.334	1.223	11.35
1236-68	33	14.2	822	1.302	1.171	12.03		9	10.6	201	1.334	0.260	31.55
1240-64	5	13.8	413	0.388	0.179	34.18	1952+29	4	15.4	297	0.427	1.187	11.82
	33	15.7	848	0.388	1.350	9.85	2002+31	4	17.6	475	2.111	-0.738	75.18
1256-67	33	15.8	1010	0.663	1.395	9.36	2016+28	4	16.0	281	0.558	-1.317	99.14
1302-64	33	17.8	1108	0.572	-1.035	89.86	2020+28	4	16.1	264	0.343	0.125	36.03
1309-53	33	14.9	306	0.728	0.852	17.06	2028+22	4	10.7	91	0.631	2.142	3.95
1309-55	33	15.8	373	0.849	4.228	0.31							
1317-53	33	15.4	338	0.280	-0.587	67.35							
1322-66	33	17.4	1185	0.543	-1.005	88.51							
1323-63	33	18.8	1265	0.793	1.496	8.35							
1323-58	33	18.6	881	0.478	-0.174	47.67							
1323-62	33	19.2	1233	0.530	0.097	37.01							
1325-49	33	11.9	187	1.479	0.639	21.40							
1336-64	33	19.0	1333	0.379	-0.931	85.00							
1352-51	33	14.5	279	0.644	-0.275	52.14							
1356-60	33	20.0	1252	0.128	-0.767	76.69							
1358-63	33	19.5	1332	0.843	-0.774	77.05							
1417-54	33	15.7	433	0.936	0.327	29.51							
1424-55	33	16.1	551	0.570	-0.390	57.52							

Table 4 lists 16 pulsars for which the predicted values of  $n_{\sigma_i}$  are greater than 5, assuming as a conservative case  $\eta I = 10 I_0$ . For this sample (total of 21 independent observations) the value of

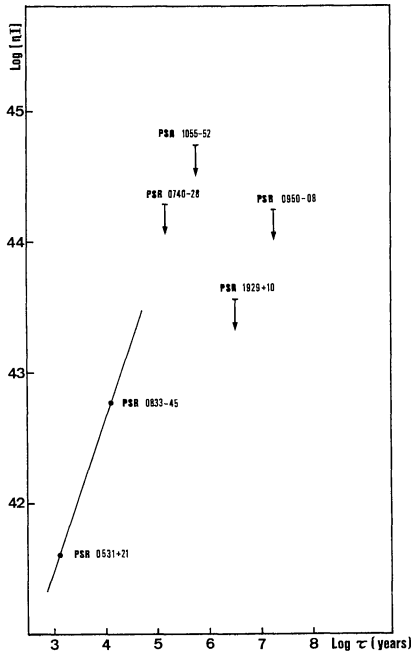
$$\alpha = -2 \ln \prod_{i=1}^{21} g_i$$

is 40.3 corresponding to a chance occurrence probability of  $\sim 50\%$ .



**Table 4.** Pulsars for which  $n_{\sigma i}$  is greater than for  $\eta I = 10I_0$ 

PSR	P(s)	P( $10^{-15}$ s/s)	d(Kpc)	$3\sigma$ upper limit flux ( $10^{-6}$ ph/cm $^2$ s)
0540+23	0.246	15.4	2.60	2.4
0611+22	0.335	59.6	3.30	1.9
0740-26	0.167	16.8	1.50	1.5
0905-51	0.253	1.8	0.86	2.7
0919+06	0.431	13.7	1.00	1.0
0950+08	0.253	0.2	0.09	1.4
1001-47	0.307	22.1	1.60	2.1
1055-52	0.197	5.8	0.92	2.2
1133+16	1.188	3.7	0.15	1.8
1449-64	0.179	2.7	2.20	3.4
1451-68	0.263	0.1	0.23	2.4
1822-09	0.769	52.3	0.56	3.7
1915+13	0.195	7.2	2.40	2.9
1916+14	1.181	211.4	0.86	2.8
1929+10	0.226	1.2	0.08	2.6
1930+22	0.144	57.8	7.00	4.1

**Fig. 2.** Plot of  $\log(\eta I)$  versus the timing age  $\tau = P/2\dot{P}$  for the pulsars predicted to have the highest visibility

There is therefore no evidence for a global signal from this sample of pulsars.

Individual results from the search for pulsation from the pulsars of Table 4 can be used to derive constraints on their values of  $\eta I$ . The situation is depicted in Fig. 2 which shows the  $3\sigma$  upper limits of  $\eta I$  for PSR1929+10, PSR1950+08, PSR0740-28, and PSR1055-52 (the pulsars with greatest  $n_{\sigma i}$ ) compared with the values of  $\eta I$  of Crab and Vela. As the figure shows there remains the possibility to accommodate an increase of the conversion efficiency  $\eta$  with the pulsar age (Harding, 1981) up to at most  $10^6$  yr.

In an adjacent energy range (15 KeV to 11 MeV) Knight et al. (1982) obtain similar conclusion although their results are not easily comparable with ours. Helfand (1983) has shown that some radio pulsars are seen as unpulsing soft X-ray sources, and that the X-ray production mechanism may be related to a  $\gamma$ -ray production mechanism.

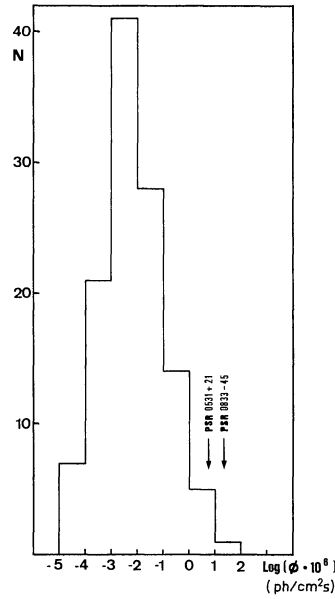
**Fig. 3.** Distribution of pulsar fluxes as expected in the case  $\eta I = 10^{4.5}$  g cm. Crab and Vela measured fluxes are shown for comparison

Figure 3 shows the distribution of expected fluxes  $\phi_i = N p_i / (\omega_i \Delta t_i)$  ( $i = 1, 117$ ) for  $\eta I = I_0$ . The observed Crab and Vela fluxes are shown for comparison. Considering that, as shown above,  $\eta I \ll I_0$  the whole distribution must be shifted to the left at least one decade. This shows that future  $\gamma$ -ray experiments (Gamma-1, GRO) will be able to detect pulsars only if their visibility threshold is improved by a factor greater than 10 with respect to COS-B.

## Discussion

A consistent theory explaining the complex phenomenology of the pulsar activity is not yet available. Synchrotron emission implies a drastic dependence of the  $\gamma$ -ray luminosity on the pulsar period ( $L_\gamma \sim P^{-4}$ ) and therefore does not predict strong  $\gamma$ -ray emission from slow pulsars. The observed dependence on the period of the  $\gamma$ -ray luminosity for the Crab and Vela pulsars has rather favoured the general framework initially proposed by Sturrock (1971) and developed by Ruderman and Sutherland (1975). In their scenario, positrons are accelerated up to very high energies ( $\sim 10^{12}$  eV) across a potential drop in an electrostatic gap in the polar caps, close to the neutron star surface. From there the particles can move along the magnetic field lines and emit  $\gamma$ -rays by the curvature radiation mechanism (Hardee, 1977; Salvati and Massaro, 1978; Ayasli, 1981). In this case the total power provided by the gap acceleration depends on the pulsar period in such a way that the conversion efficiency  $\eta$  increases with the pulsar age (Buccheri et al., 1978; Harding, 1981). For the range of ages dealt with in this paper it is not possible to rely on these theoretical expectations in view of the negative results of the present analysis. It will be assumed that the value of  $\eta$  does not change very much within our sample in order to derive an upper limit on its average value.

To do so, consider the statistical variable

$$N_\sigma = \frac{\sum_{i=1}^{21} n_{\sigma i}}{\sqrt{21}} \quad (8)$$

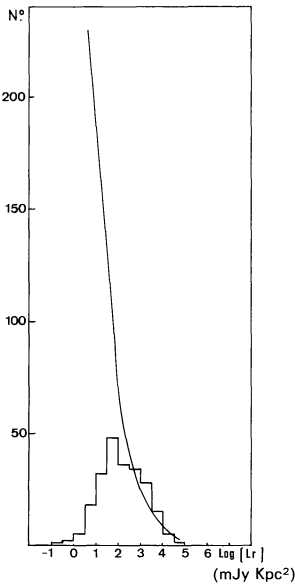


**Fig. 4.** Distribution of the radio luminosity for 224 detected pulsars fitted with the luminosity distribution obtained after removal of selection effects

based on the 16 pulsars of the priority list (Table 4). According to the Central Limit Theorem,  $N_\sigma$  has a gaussian p.d.f. Substituting in (8) relation (7) for  $n_{\sigma i}$  and putting  $N_\sigma = 3$ , a  $3_\sigma$  upper limit is obtained on the average value of  $\eta I$  of our sample. This is

$$(\eta I)_{3\sigma} < 0.06 \cdot 10^{4.5} \text{ g cm}^2. \quad (9)$$

It is now possible to estimate an upper limit on the contribution of pulsars ( $L_{\gamma t}$ ) to the observed galactic  $\gamma$ -ray emission. For  $I = I_0$

$$L_{\gamma t} < 0.06 \langle \dot{E} \rangle \times N \quad (\text{ergs/s}),$$

where  $\langle \dot{E} \rangle$  is the average value of  $\dot{E}$  over the  $N = 500,000$  pulsars of the galaxy (Lyne, 1981). The estimate of  $\langle \dot{E} \rangle$  presents some difficulties. The value calculated using the MT catalogue is not representative of the whole population of pulsars due to selection effects against low luminosity pulsars which are seen only when they are very near to the earth. A correction is however possible by using the radio luminosity distributions given by Lyne (1981). From these distributions one can estimate the number of low luminosity pulsars missed in the published surveys and necessary to render complete the MT catalogue with respect to the radio luminosity. The observed luminosity distribution of 224 pulsars is fitted on the high luminosity side with the luminosity distribution derived by Lyne (1981) after elimination of the selection effects (Fig. 4). The agreement on the low luminosity side can be obtained by adding  $N_u \sim 1400$  “undetected” radio pulsars with an average radio luminosity of  $L_r = 2.6 \cdot 10^{26} \text{ erg/s}$ . From the MT catalogue it is found that this value for the radio luminosity corresponds approximately to an average value of  $\dot{E}$  equal to

$$\langle E_u \rangle = 4.6 \cdot 10^{32} \text{ erg/s}.$$

Thus

$$\langle \dot{E} \rangle = \frac{N_u \langle E_u \rangle + N_d \langle \dot{E}_d \rangle}{N_d + N_u} = 1.3 \cdot 10^{33} \text{ erg/s},$$

where  $\langle \dot{E}_d \rangle = 6.7 \cdot 10^{33} \text{ erg/s}$  is the average value of  $\dot{E}$  computed from the  $N_d = 224$  “detected” pulsars of the MT catalogue. This implies

$$L_{\gamma t} < 4.0 \cdot 10^{37} \text{ erg/s}$$

or

$$L_{\gamma t} < 13 \cdot 10^{40} \text{ ph/s}$$

in the energy range 50 MeV to 2 GeV.

Caraveo and Paul (1979) have derived for the total galactic  $\gamma$ -ray emission above 100 MeV the value  $1.2 \cdot 10^{42} \text{ ph/s}$ ; for a  $E^{-2}$  spectrum, this is  $2.4 \cdot 10^{42} \text{ ph/s}$  above 50 MeV so that the pulsar contribution in this energy range is less than 5%.

This result disagrees with previously published results derived on a theoretical basis (e.g. Salvati and Massaro, 1982; Harding and Stecker, 1981). It is therefore of particular importance in setting up theoretical models aiming to predict  $\gamma$ -ray emission from slow pulsars. The  $\gamma$ -ray luminosity law as derived from Crab and Vela cannot extend beyond  $\sim 40,000 \text{ yr}$  suggesting a distinction between young and old pulsars in  $\gamma$ -rays. While old pulsars cannot account for a significant fraction of the observed galactic  $\gamma$ -ray emission, young undetected pulsars may be more important. They remain plausible counterparts of the galactic  $\gamma$ -ray sources (Buccheri et al., 1981) which are believed to contribute a significant fraction to the galactic  $\gamma$ -ray emission (e.g. Bignami et al., 1978).

**Acknowledgements.** The authors wish to express appreciation to their friend and colleague Ray Wills whose significant efforts throughout all phases of the COS-B mission have been an important factor of success.

M.E.Ö. acknowledges receipt of Alexander-von-Humboldt fellowship. The authors are grateful to Dr. I. I. Shapiro for making available the MIT barycentric ephemeris.

## References

- Arons, J., Scharlemann, E.T.: 1979, *Astrophys. J.* **231**, 854
- Ayasli, S.: 1981, *Astrophys. J.* **249**, 698
- Bendat, J.S., Piersol, A.G.: 1971, *Random Data: Analysis and Measurement procedures*, Wiley, New York
- Bignami, G.F., Caraveo, P.A., Maraschi, L.: 1978, *Astron. Astrophys.* **67**, 149
- Buccheri, R., D’Amico, N., Kanbach, G., Masnou, J.L., Scarsi, L.: 1977, *Proc. 12th ESLAB Symp. Recent Advances in  $\gamma$ -ray Astronomy*, ESA SP-124, p. 309
- Buccheri, R., D’Amico, N., Massaro, E., Scarsi, L.: 1978, *Nature* **274**, 572
- Buccheri, R.: 1981, *IAU Symp.* **95**, “Pulsars”, Reidel, Dordrecht, p. 241
- Buccheri, R., Morini, M., Sacco, B.: 1981, *Phil. Trans. Roy. Soc. London*, **A301**, 495
- Caraveo, P.A., Paul, J.A.: 1979, *Astron. Astrophys.* **75**, 340
- Eadie, A.T., Drijard, D., James, F.E., Roos, M., Sadoulet, B.: 1971, *Statistical Methods in Experimental Physics*, North-Holland, Amsterdam
- Ferguson, D., Boriakoff, V.: 1980, *Astrophys. J.* **239**, 310
- Gerardi, G., Buccheri, R., Sacco, B.: 1982, *COMPSTAT 82*, Toulouse, August–September
- Gullahorn, G.E., Rankin, M.J.: 1978, *Astron. J.* **83**, 1219
- Hardee, P.E.: 1977, *Astrophys. J.* **216**, 873
- Harding, A.K.: 1981, *Astrophys. J.* **245**, 267

- Harding, A.K., Stecker, F.W.: 1981, *Nature* **290**, 316
- Helfand, D.J.: 1983, in *Supernova Remnants and their X-ray emission*, IAU Symp. **101**, eds. P. Gorenstein and J. Danziger (in press)
- Kanbach, G., Bennett, K., Bignami, G.F., Boella, G., Bonnardeau, M., Buccheri, R., D'Amico, N., Hermesen, W., Hidgon, J.C., Lichti, G.G., Masnou, J.L., Mayer-Hasselwander, H.A., Paul, J.A., Scarsi, L., Swanenburg, B.N., Taylor, B.G., Wills, R.D.: 1977, Proc. of 12th ESLAB Symp., Recent Advances in  $\gamma$ -ray Astronomy, ESA SP-124, p. 21
- Knight, F.K., Matteson, J.L., Peterson, L.E., Rothschild, R.E.: 1982, *Astrophys. J.* **260**, 553
- Lyne, A.G.: 1981, in *Pulsars*, IAU Symp. **95**, Reidel, Dordrecht, p. 423
- Manchester, R.N., Taylor, J.H.: 1981, *Astron. J.* **86**, 1953
- Manchester, R.N., Newton, L.M., Goss, W.M., Hamilton, P.A.: 1983, *Monthly Notices Roy. Astron. Soc.* **202**, 269
- Mayer-Hasselwander, H.A., Bennett, K., Bignami, G.F., Buccheri, R., Caraveo, R.A., Hermesen, W., Kanbach, G., Lebrun, F., Lichti, G.G., Masnou, J.L., Paul, J.A., Pinkau, K., Sacco, B., Scarsi, L., Swanenburg, B.N., Wills, R.D.: 1982, *Astron. Astrophys.* **105**, 164
- Moszkowski, S.: 1974, *Phys. Rev. D* **9**, 1613
- Newton, L.M., Manchester, R.N., Cooke, D.J.: 1981, *Monthly Notices Roy. Astron. Soc.* **194**, 841
- Ögelman, H., Fichtel, C.E., Kniffen, D.A., Thompson, D.J.: 1976, *Astrophys. J.* **209**, 584
- Ruderman, M.A., Sutherland, P.G.: 1975, *Astrophys. J.* **196**, 51
- Salvati, M., Massaro, E.: 1978, *Astron. Astrophys.* **67**, 55
- Salvati, M., Massaro, E.: 1982, *Monthly Notices Roy. Astron. Soc.* **198**, 11
- Scarsi, L., Bennett, K., Bignami, G.F., Boella, G., Buccheri, R., Hermesen, W., Koch, L., Mayer-Hasselwander, H.A., Paul, J.A., Pfeffermann, E., Stiglitz, R., Swanenburg, B.N., Taylor, B.G., Wills, R.D.: 1977, Proc. of 12th ESLAB Symp., Recent Advances in  $\gamma$ -ray Astronomy, ESA SP-124, p. 3
- Sturrock, P.A.: 1971, *Astrophys. J.* **164**, 529
- Thompson, D.J., Fichtel, C.E., Kniffen, D.A., Lamb, D.C., Ögelman, H.B.: 1976, *Astrophys. Letters* **17**, 173
- Van de Hulst, H.C., Scheepmaker, A., Swanenburg, B.N., Mayer-Hasselwander, H.A., Pfeffermann, E., Pinkau, K., Rothermel, H., Schneider, H., Voges, W., Labeyrie, J., Keirle, P., Paul, J., Bellomo, G., Bignami, G., Boella, G., Scarsi, L., Hutchinson, G.W., Pearce, A.J., Ramsden, D., Wills, R.D., Wright, P.J.: 1971, *New Technique in Space Astronomy*, Proc. IAU Symp. **41**, p. 37
- Wills, R.D., Bennett, K., Bignami, G.F., Buccheri, R., Caraveo, P.A., Hermesen, W., Kanbach, G., Masnou, J.L., Mayer-Hasselwander, H.A., Paul, J.A., Sacco, B.: 1981, Proc. of 17th ICRC, Paris